AMERICAN SOCIETY FOR MICROBIOLOGY | Molecular and Cellular Biology®

RESEARCH ARTICLE

Glucocorticoid Receptor Accelerates, but Is Dispensable for, Adipogenesis

Young-Kwon Park, Kai Ge

Adipocyte Biology and Gene Regulation Section, LERB, National Institute of Diabetes and Digestive and Kidney Diseases, National Institutes of Health, Bethesda, Maryland, USA

ABSTRACT Dexamethasone (DEX), a synthetic ligand for glucocorticoid receptor (GR), is routinely used to stimulate adipogenesis in culture. GR-depleted preadipocytes show adipogenesis defects 1 week after induction of differentiation. However, it has remained unclear whether GR is required for adipogenesis *in vivo*. By deleting *GR* in precursors of brown adipocytes, we found unexpectedly that GR is dispensable for brown adipose tissue development in mice. In culture, GR-deficient primary or immortalized white and brown preadipocytes showed severely delayed adipogenesis 1 week after induction of differentiation. However, when differentiation was extended to 3 weeks, GR-deficient preadipocytes showed levels of adipogenesis marker expression and lipid accumulation similar to those of the wild-type cells, indicating that DEX-bound GR accelerates, but is dispensable for, adipogenesis. Consistently, DEX accelerates, but is dispensable for, adipogenesis in culture. We show that DEX-bound GR accelerates adipogenesis by directly promoting the expression of adipogenic transcription factors CCAAT/enhancer-binding protein alpha (C/EBPα), C/EBPβ, C/EBPδ, KLF5, KLF9, and peroxisome proliferator-activated receptor γ (PPARγ) in the early phase of differentiation. Mechanistically, DEX-bound GR recruits histone H3K27 acetyltransferase CBP to promote activation of C/EBPβ-primed enhancers of adipogenic genes. These results clarify the role of GR in adipogenesis *in vivo* and demonstrate that DEX-mediated activation of GR accelerates, but is dispensable for, adipogenesis.

KEYWORDS GR, adipogenesis, dexamethasone, glucocorticoid receptor

Received 3 May 2016 **Returned for modification** 19 May 2016 **Accepted** 18 October 2016

Accepted manuscript posted online 24 October 2016

Citation Park Y-K, Ge K. 2017. Glucocorticoid receptor accelerates, but is dispensable for, adipogenesis. Mol Cell Biol 37:e00260-16. https://doi.org/10.1128/MCB.00260-16.

Address correspondence to Kai Ge, kai.ge@nih.gov.

For a companion article on this topic, see https://doi.org/10.1128/MCB00554-16.

Synthetic glucocorticoids, including dexamethasone (DEX), are widely prescribed in clinics to treat inflammatory and autoimmune diseases. Endogenous and synthetic glucocorticoids function as ligands for glucocorticoid receptor (GR, also known as Nr3c1), which is a member of the nuclear receptor family of transcription factors (TFs). Glucocorticoids bind to the ligand-binding domain of GR in the cytoplasm and cause it to translocate to the nucleus by releasing GR form chaperone proteins. Once in the nucleus, GR directly binds to transcriptional enhancers and recruits chromatin-modifying enzymes to activate target gene expression (1).

DEX is routinely used to stimulate differentiation of preadipocytes, including the widely used white preadipocyte cell line 3T3-L1 in culture (2–4). Adipogenesis is initiated by treating postconfluent 3T3-L1 preadipocytes with the adipogenic cocktail consisting of isobutylmethylxanthine (IBMX), DEX, and insulin, collectively known as MDI, for 2 days, followed by maintaining cells in culture medium without the adipogenic cocktail for an additional 4 to 6 days (4). DEX-bound GR promotes 3T3-L1 adipogenesis through at least two mechanisms. First, DEX-bound GR rapidly and directly induces expression of early adipogenic TF CCAAT/enhancer-binding protein delta (C/EBPδ) within hours of induction of adipogenesis (5, 6). Second, upon stimulation with MDI, GR and another early adipogenic TF, C/EBPβ, transiently associate with histone acetyltransferase p300 and induce histone H3 acetylation and activation of

enhancers of many adipogenic genes, including the master adipogenic TF peroxisome proliferator-activated receptor γ (PPARγ) (7). C/EBPβ functions as a pioneering TF to facilitate the genomic binding of GR to enhancer regions (8).

It has been shown that small interfering RNA (siRNA)-mediated knockdown of GR in 3T3-L1 cells prevents the accumulation of lipid droplets and expression of adipocyte-selective proteins 8 days after induction of differentiation (7). On the other hand, immortalized *GR* knockout (KO) brown preadipocytes show delayed adipogenesis, which ultimately catches up to that of wild-type cells (9). However, the importance of glucocorticoid-mediated activation of GR for adipogenesis *in vivo* has not been shown (10). In this paper, we have investigated the role of endogenous GR in adipogenesis by employing conditional KO mice and derived white and brown preadipocytes. By deleting the *GR* gene in precursor cells of brown fat, we found that surprisingly, GR is largely dispensable for brown adipose tissue (BAT) development in mice. By deleting the *GR* gene in primary or immortalized white and brown preadipocytes, we found that DEX-mediated activation of GR accelerates, but is largely dispensable for, adipogenesis in culture. Mechanistically, DEX-bound GR recruits H3K27 acetyltransferase CBP to promote activation of C/EBPβ-primed enhancers of adipogenic genes.

RESULTS

GR is largely dispensable for BAT development. To understand the role of GR in adipose tissue development, we generated $GR^{f/f}$; *Myf5-Cre* (conditional KO [cKO]) mice by crossing $GR^{f/f}$ mice with *Myf5-Cre* mice. Myf5-Cre specifically deletes genes flanked by loxP sites in somitic precursor cells giving rise to both BAT and skeletal muscles in the back (11). Littermate $GR^{f/f}$ (f/f) mice were used as the control. cKO pups were obtained at the expected Mendelian ratio, and all survived beyond 6 weeks after birth without any obvious developmental defect (Fig. 1A and B). Various white adipose tissues (WATs) and BATs were isolated from 6-week-old adult mice. To our surprise, all tissues examined, including BAT, showed similar sizes and morphologies for cKO and control mice (Fig. 1C and D). Consistent with the phenotype, deletion of *GR* in BAT had little effect on expression of adipogenesis markers *Pparγ*, *Cebpα*, and *Fabp4* as well as BAT markers *Prdm16* and *Ucp1* (Fig. 1E). Embryonic day 18.5 (E18.5) cKO and f/f embryos were also indistinguishable (Fig. 1F). Deletion of *GR* gene by Myf5-Cre in E18.5 BAT was confirmed by PCR quantification of genomic DNA (Fig. 1G). Histological analyses of the interscapular area revealed similar morphologies of BATs and muscles for cKO and control embryos (Fig. 1H). Gene expression analysis by RNA sequencing (RNA-Seq) showed that only a small number of genes increased (0.7%) or decreased (0.6%) over 2-fold in cKO compared with control E18.5 BAT (Fig. 1I). RNA-Seq also confirmed the deletion of exon 2 of *GR* gene in cKO samples (Fig. 1J). Consistent with data from adult mice, *GR* deletion had little effect on the expression of adipogenesis and BAT markers in E18.5 BATs (Fig. 1K). RNA-Seq data also showed that *GR* deletion did not affect adipogenic gene expression in E18.5 BATs, although several genes involved in thermogenesis such as *Dio2* and *Elovl3* decreased moderately (Fig. 1L).

To investigate the functional consequence of *GR* deletion in BATs, we acutely exposed cKO mice to environmental cold (4°C). cKO mice maintained normal body temperatures, were cold tolerant, and displayed a behavior similar to that of control mice in the cold tolerance test (Fig. 2A). The expression of the major thermogenic gene *Ucp1* was similarly induced by cold exposure in BATs of cKO and control mice (Fig. 2B). The expression levels of *Dio2* and *Elovl3* after cold exposure were less in BATs of cKO mice, which is likely due to the moderately reduced basal levels by *GR* deletion in adult mice and embryos housed at room temperature (Fig. 1L and 2B). Nevertheless, these results suggest that GR is largely dispensable for BAT function. Taken together, while a full physiological characterization of $GR^{f/f}$; *Myf5-Cre* mice needs to be done in the future, these data indicate that GR is largely dispensable for BAT development in mice.

GR accelerates, but is dispensable for, adipogenesis in culture. Our finding that GR is largely dispensable for BAT development appeared to be inconsistent with the previous observation that knockdown of GR in 3T3-L1 cells impaired adipogenesis in

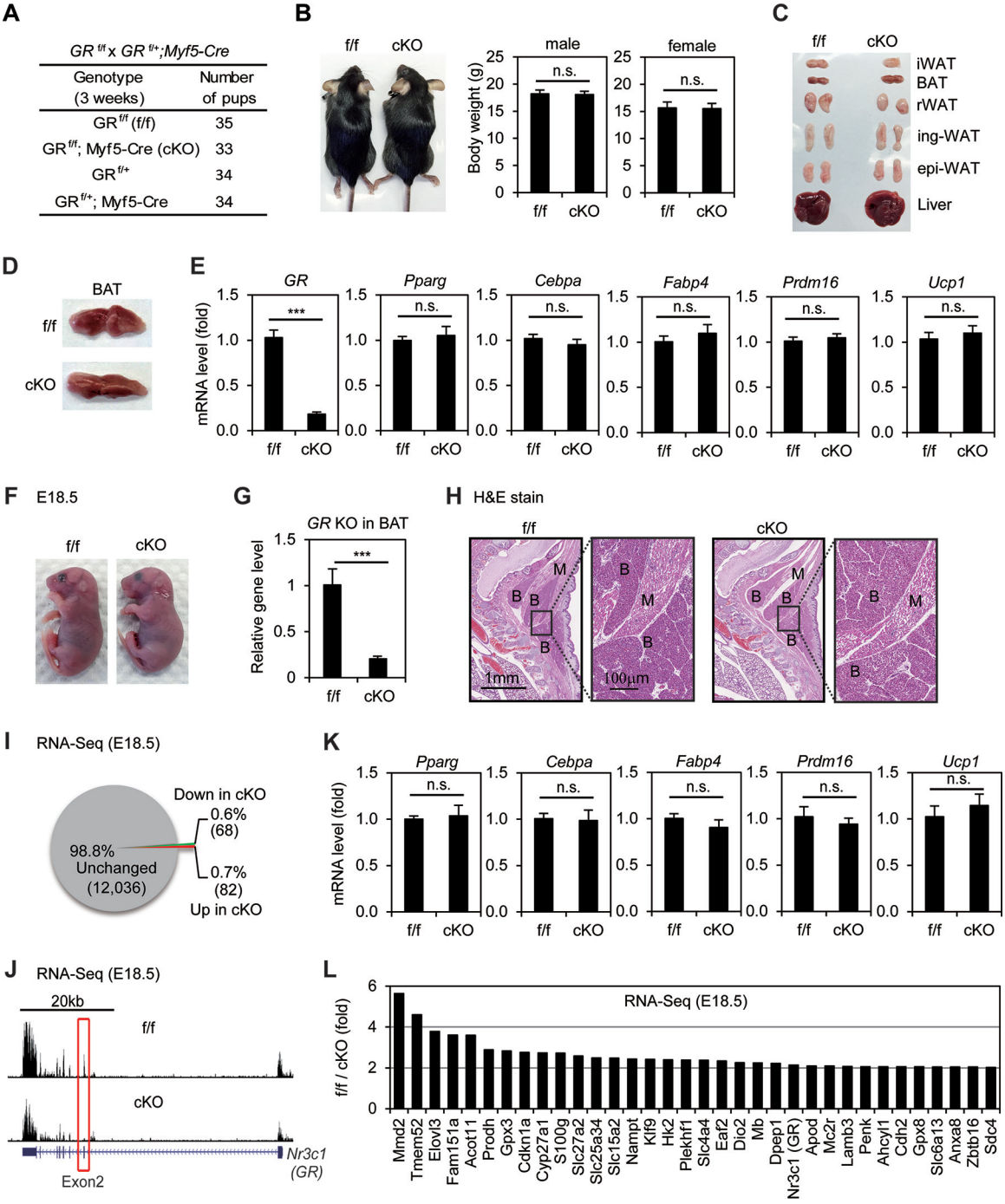

FIG 1 GR is largely dispensable for BAT development. $GR^{f/f}$ mice were crossed with $GR^{f/+}$; *Myf5-Cre* mice to obtain $GR^{f/f}$; *Myf5-Cre* (conditional KO, cKO) and littermate control ($GR^{f/f}$, f/f) mice and embryos. (A to E) Characterization of $GR^{f/f}$; *Myf5-Cre* adult mice. (A) Genotyping results. The expected ratios of the four genotypes are 1:1:1:1. (B) Representative pictures of male mice (left panel) and body weight of f/f ($n = 9$) or cKO ($n = 12$) mice (right panel). (C) Pictures of isolated adipose tissues. iWAT, interscapular WAT; epi-WAT, epididymal WAT; ing-WAT, inguinal WAT; rWAT, retroperitoneal WAT. (D) Representative pictures of interscapular BAT. (E) Total RNA was extracted from BAT of f/f ($n = 9$) or cKO ($n = 12$) mice for qRT-PCR analysis of *GR*, adipogenesis markers *Pparγ*, *Cebpα*, and *Fabp4* as well as BAT markers *Prdm16* and *Ucp1*. Quantitative PCR data in all figures are presented as means ± SEM. ***, $P < 0.001$. n.s., no significance. (F to L) Characterization of $GR^{f/f}$; *Myf5-Cre* E18.5 embryos. (F) Representative pictures of E18.5 embryos. (G) Confirmation of *GR* deletion in E18.5 BAT by qPCR analysis of genomic DNA. (H) E18.5 embryos were sagittally sectioned along the midline. Sections of the interscapular area were stained with hematoxylin and eosin (H&E). B, BAT; M, muscle. (I) RNA-Seq analysis of BAT collected from two E18.5 *GR* cKO embryos. Pie chart depicts genes up- or downregulated in cKO samples. The threshold for up- or downregulation is 2-fold. (J) The genome browser view shows the deletion of exon 2 of *GR* gene in cKO samples. (K) RNA was extracted from E18.5 BAT of f/f ($n = 4$) or cKO ($n = 8$) embryos for qRT-PCR analysis. (L) List of the most significantly downregulated mRNAs in E18.5 BAT of *GR* cKO embryos. Only genes with expression levels with an RPKM of >3.3 in the f/f BATs were included.

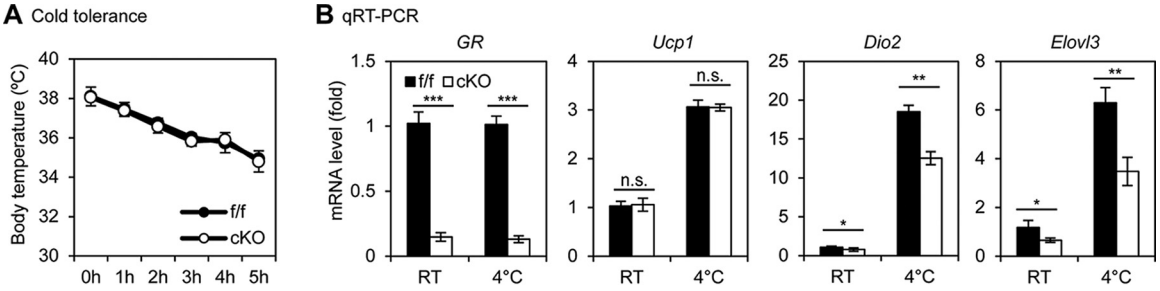

FIG 2 Cold tolerance test of $GR^{f/f}$; *Myf5-Cre* mice. (A) Body temperatures of $GR^{f/f}$; *Myf5-Cre* (cKO) and their littermate control (f/f) mice (n = 5 per group) after acute exposure to 4°C for 5 h. Body temperatures were measured every hour. (B) qRT-PCR analysis of thermogenic genes in BAT. RT, room temperature. Data are presented as means ± SEM. *, $P < 0.05$; **, $P < 0.01$; ***, $P < 0.001$. n.s., no significance.

culture (7). To explain these paradoxical observations, we tested whether deletion of *GR* in preadipocytes would affect adipogenesis in culture. For this purpose, primary preadipocytes isolated from BAT of newborn $GR^{f/f}$ pups were immortalized with SV40 large T antigen (SV40T). Cells were infected with retroviral Cre to stably delete *GR* gene (Fig. 3A). Consistent with the previous report for 3T3-L1 cells (7), depletion of GR severely impaired adipogenesis and induction of adipocyte genes at day 7 (D7) of differentiation (Fig. 3B and C and 4A). RNA-Seq analyses showed that GR-dependent upregulated genes at D7 were functionally associated strongly with fat cell differentiation, although GR-dependent upregulated genes at day 2 (D2) were associated mainly with the inflammatory response (Fig. 4B and C). The adipogenesis defects observed at D7 of differentiation in *GR* KO cells could be prevented by ectopic expression of either PPARγ or C/EBPβ (Fig. 5), which works downstream of GR during preadipocyte differentiation.

Interestingly, when we extended the differentiation process to day 14 (D14) and day 21 (D21), we observed much less severe morphological differences between *GR* KO and wild-type cells (Fig. 3B). Consistently, deletion of *GR* significantly decreased the induction of adipogenesis markers *Ppar*γ, *Cebp*α, and *Fabp4* as well as BAT marker *Ucp1* at D7 but not at D21 of adipogenesis (Fig. 3C). In 3T3-L1 white preadipocytes, stable knockdown of *GR* by short hairpin RNA (shRNA) led to severe adipogenesis defects at D7 of differentiation, confirming the previous report (7). However, extending differentiation to D21 largely rescued the differentiation in 3T3-L1 cells (Fig. 3D to F). GR-depleted cells displayed moderately reduced lipid accumulation at D21 of adipogenesis (Fig. 3B and E), which was likely due to the moderately decreased expression of major lipogenic genes such as *Stearoyl Coenzyme A desaturase 1* (*Scd1*), *Sterol regulatory element binding transcription factor 1* (*Srebp1c*), *Fatty acid synthase* (*Fasn*), and *Liver X receptor* α (*Lxr*) in these SV40T-immortalized brown and white adipocytes (Fig. 3C and F).

Similar to our observations in immortalized preadipocytes, deletion of *GR* in primary white and brown preadipocytes decreased the induction of adipogenesis markers at D7 but not at D21 of differentiation (Fig. 6A to D). Unlike immortalized preadipocytes, *GR* KO primary white and brown preadipocytes showed levels of *Fasn* and *Lxr* expression and lipid accumulation at D21 of differentiation similar to those of wild-type cells, indicating that GR is dispensable for adipogenesis of primary preadipocytes. Mature brown adipocytes collected at D21 of differentiation were treated by CL316,243, a selective adrenergic-β3 receptor agonist. As shown in Fig. 6E, deletion of *GR* had little effect on CL316,243-induced expression of *Ucp1* in brown adipocytes. Together, these data indicate that GR accelerates, but is dispensable for, adipogenesis in culture.

DEX accelerates, but is dispensable for, adipogenesis in culture. Our observation that GR accelerates, but is dispensable for, adipogenesis in culture suggests a possibility that GR ligand DEX is also dispensable for adipogenesis. To test this possibility, confluent wild-type brown preadipocytes were treated with adipogenic cocktail with or without DEX for 2 days and then maintained in the differentiation

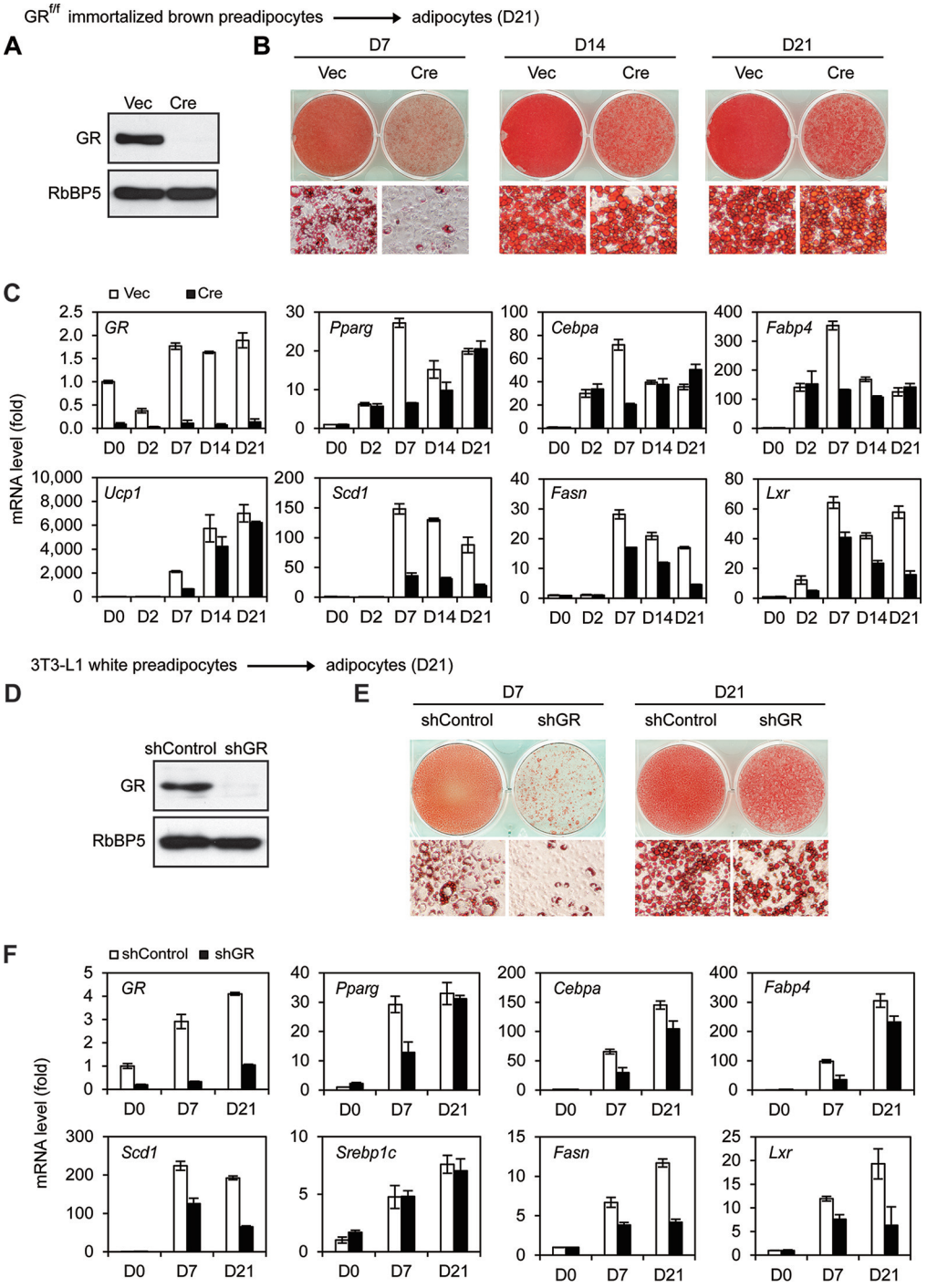

FIG 3 GR accelerates, but is largely dispensable for, adipogenesis and induction of master adipogenic TFs. (A to C) *GR*$^{f/f}$ immortalized brown preadipocytes were infected with retroviral vector MSCVpuro expressing Cre, followed by brown adipogenesis assays. (A) Whole-cell lysates were subjected to Western blot analysis of GR in preadipocytes. RbBP5 was used as a loading control. Vec, vector. (B) Oil Red O staining of differentiated cells at day 7 (D7) and day 21 (D21). Upper panels, stained dishes; lower panels, representative fields under the microscope. (C) qRT-PCR analysis of gene expression at indicated time points of brown adipogenesis. (D to F) 3T3-L1 white preadipocytes were infected with lentiviral vector expressing control (shControl) or GR knockdown shRNA (shGR), followed by adipogenesis assays. (D) Western blot analysis of GR in preadipocytes. (E) Oil Red O staining of differentiated cells at D7 and D21. (F) qRT-PCR analysis of gene expression.

medium for 3 weeks. As shown in Fig. 7, omission of DEX from the adipogenic cocktail impaired adipogenesis and induction of adipocyte marker genes at D7 of differentiation. However, extending differentiation to D21 largely rescued adipogenesis. These data indicate that DEX accelerates, but is dispensable for, adipogenesis in culture.

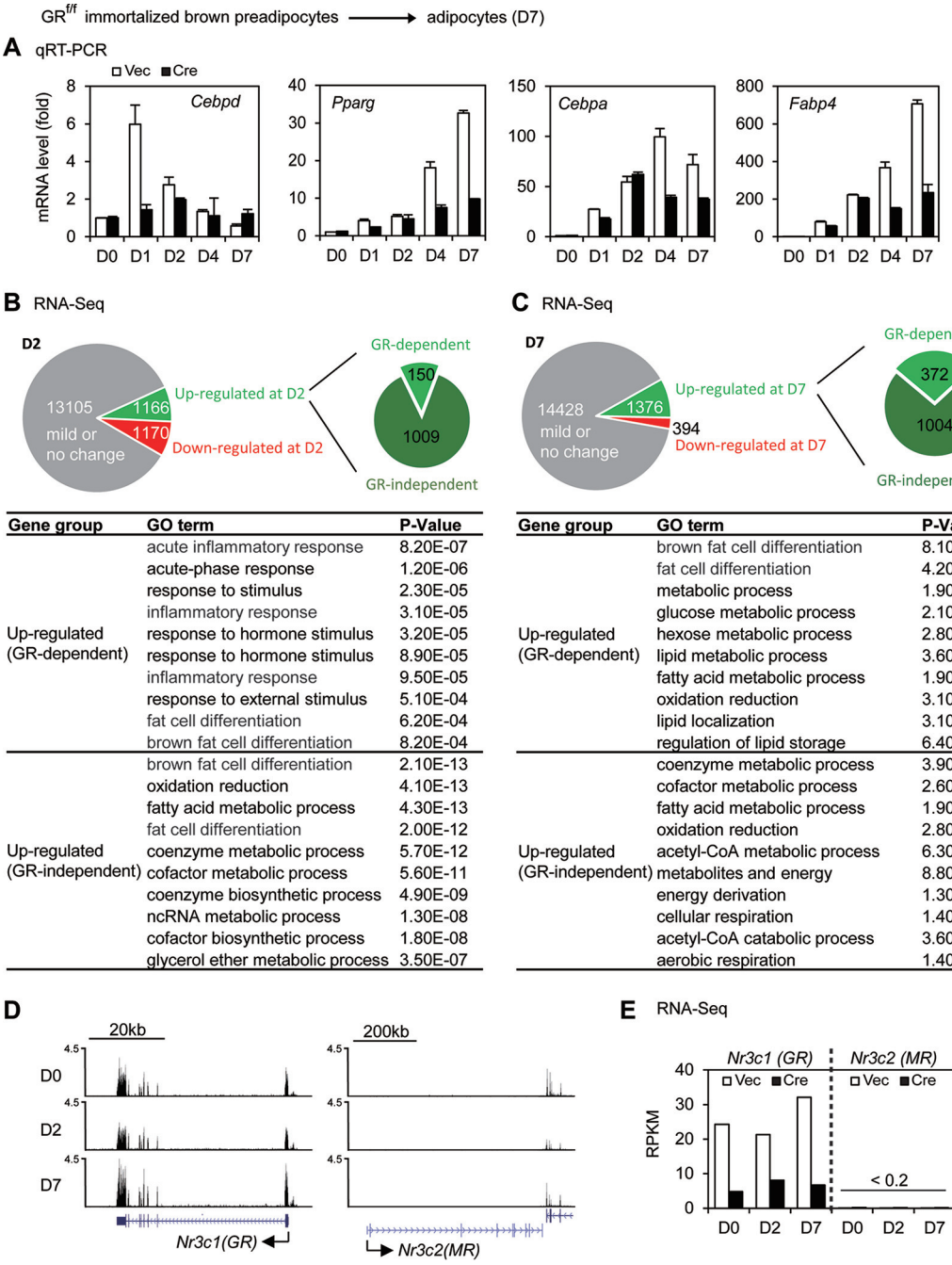

Gene group	GO term	P-Value
Up-regulated (GR-dependent)	acute inflammatory response	8.20E-07
	acute-phase response	1.20E-06
	response to stimulus	2.30E-05
	inflammatory response	3.10E-05
	response to hormone stimulus	3.20E-05
	response to hormone stimulus	8.90E-05
	inflammatory response	9.50E-05
	response to external stimulus	5.10E-04
	fat cell differentiation	6.20E-04
	brown fat cell differentiation	8.20E-04
Up-regulated (GR-independent)	brown fat cell differentiation	2.10E-13
	oxidation reduction	4.10E-13
	fatty acid metabolic process	4.30E-13
	fat cell differentiation	2.00E-12
	coenzyme metabolic process	5.70E-12
	cofactor metabolic process	5.60E-11
	coenzyme biosynthetic process	4.90E-09
	ncRNA metabolic process	1.30E-08
	cofactor biosynthetic process	1.80E-08
	glycerol ether metabolic process	3.50E-07

Gene group	GO term	P-Value
Up-regulated (GR-dependent)	brown fat cell differentiation	8.10E-26
	fat cell differentiation	4.20E-22
	metabolic process	1.90E-09
	glucose metabolic process	2.10E-09
	hexose metabolic process	2.80E-09
	lipid metabolic process	3.60E-08
	fatty acid metabolic process	1.90E-05
	oxidation reduction	3.10E-05
	lipid localization	3.10E-05
	regulation of lipid storage	6.40E-05
Up-regulated (GR-independent)	coenzyme metabolic process	3.90E-20
	cofactor metabolic process	2.60E-18
	fatty acid metabolic process	1.90E-16
	oxidation reduction	2.80E-16
	acetyl-CoA metabolic process	6.30E-13
	metabolites and energy	8.80E-10
	energy derivation	1.30E-09
	cellular respiration	1.40E-09
	acetyl-CoA catabolic process	3.60E-09
	aerobic respiration	1.40E-08

FIG 4 GR accelerates adipocyte gene induction during 7-day adipogenesis in culture. *GR*$^{f/f}$ immortalized brown preadipocytes were infected with MSCVpuro expressing Cre. Cells were collected at the indicated time points during brown adipogenesis for analyses of gene expression using qRT-PCR (A) and RNA-Seq (B to D). (A) Expression of adipogenesis markers at indicated time points. (B and C) Upper panels, schematic pie charts depict GR-dependent and -independent upregulated genes at day 2 (D2) and D7. The threshold for determining up- or downregulation is 2.5-fold. Lower panels, gene ontology (GO) analysis of gene groups defined in upper panels. GO terms with *P* values of ≤1E−4 for each group of genes are listed. ncRNA, noncoding RNA; acetyl-CoA, acetyl coenzyme A. (D and E) The mRNA levels of *GR* and *Mineralocorticoid receptor* (*MR*) during brown adipogenesis were determined by RNA-Seq. (D) RNA-Seq profiles of *GR* and *MR*. (E) RPKM values of *GR* and *MR* in *GR* KO cells. RPKM values indicate gene expression levels.

GR directly activates expression of multiple adipogenic TFs. To understand how GR accelerates adipogenesis in culture, we compared gene expression at 0 h and 4 h of differentiation by RNA-Seq. We chose 4 h because extensive chromatin opening and establishment of TF "hot spots" occur at this time point (8). We found that 752 genes were upregulated >2.5-fold from 0 h to 4 h. Among them, 247 were upregulated in a

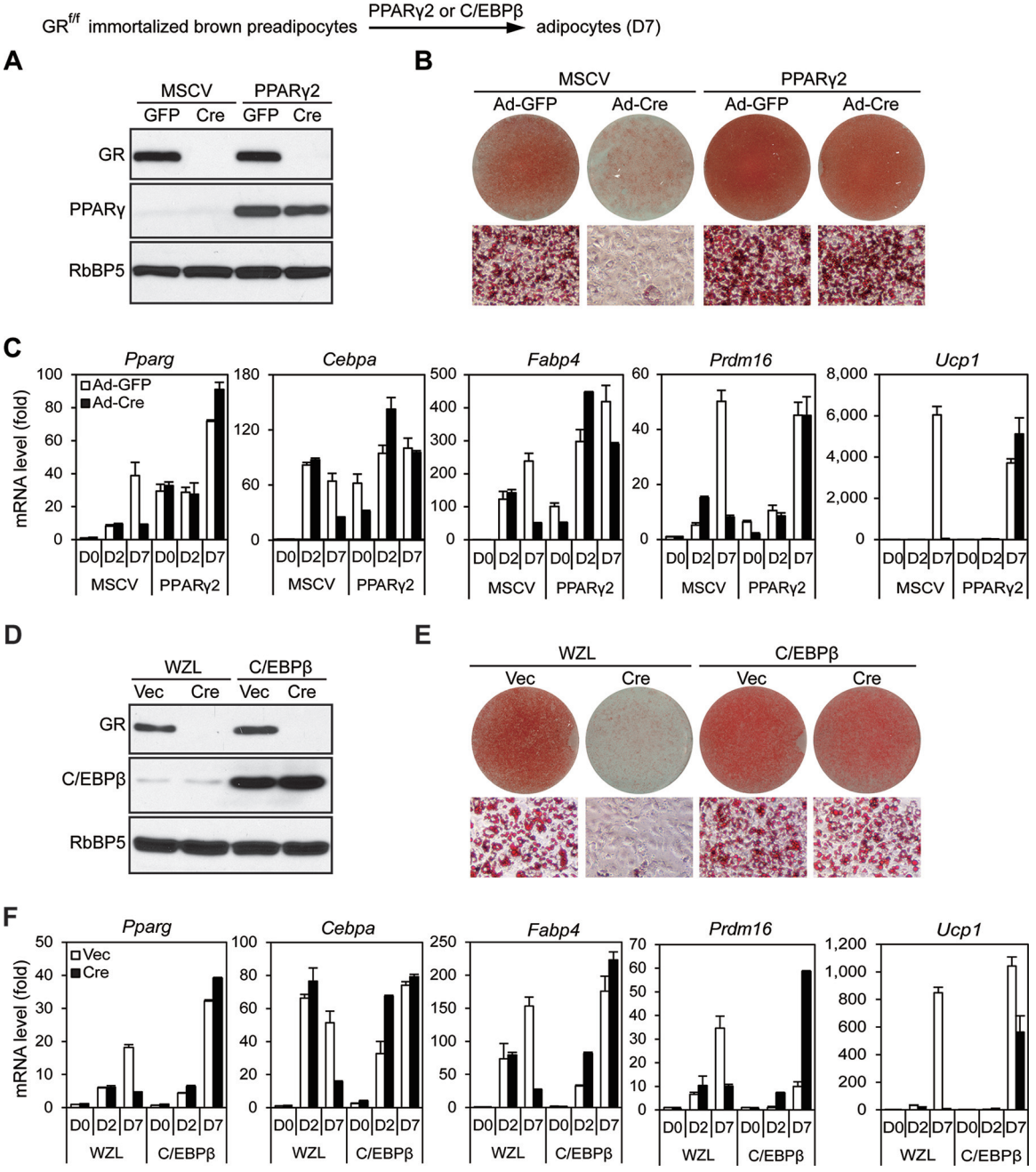

FIG 5 GR is dispensable for PPARγ- or C/EBPβ-stimulated adipogenesis. *GR*$^{f/f}$ immortalized brown preadipocytes were infected with retroviral vector MSCVhygro expressing PPARγ or WZLhygro expressing C/EBPβ. After hygromycin selection, cells were infected with adenoviruses expressing green fluorescent protein (GFP) (Ad-GFP) or Cre (Ad-Cre) for PPARγ-expressing cells or with MSCVpuro expressing vector (Vec) or Cre for C/EBPβ-expressing cells. Adipogenesis were induced for 7 days. (A and D) Western blot analysis for confirming deletion of GR and ectopic expression of PPARγ (A) or C/EBPβ (D) in preadipocytes, respectively. RbBP5 was used as a loading control. (B and E) Oil Red O staining of differentiated cells at D7. (C and F) qRT-PCR analysis of gene expression.

GR-dependent manner (Fig. 8A). An examination of the list of 247 genes identified adipogenic TFs C/EBPβ, C/EBPδ, Klf5, and Klf9 (Fig. 8B), all of which have been shown to promote adipogenesis in culture (5, 12). GR-dependent induction of these adipogenic TFs in the early phase of adipogenesis was confirmed by reverse transcription-quantitative PCR (qRT-PCR) (Fig. 8C). By chromatin immunoprecipitation sequencing (ChIP-seq) analyses at 0 h and 4 h using a GR-specific antibody, we observed GR binding on or near *Cebpβ*, *Cebpδ*, *Klf5*, *Klf9*, *Cebpα*, and *Pparγ* gene loci at 4 h but not at 0 h of adipogenesis (Fig. 8D). Thus, at least one of the mechanisms by which

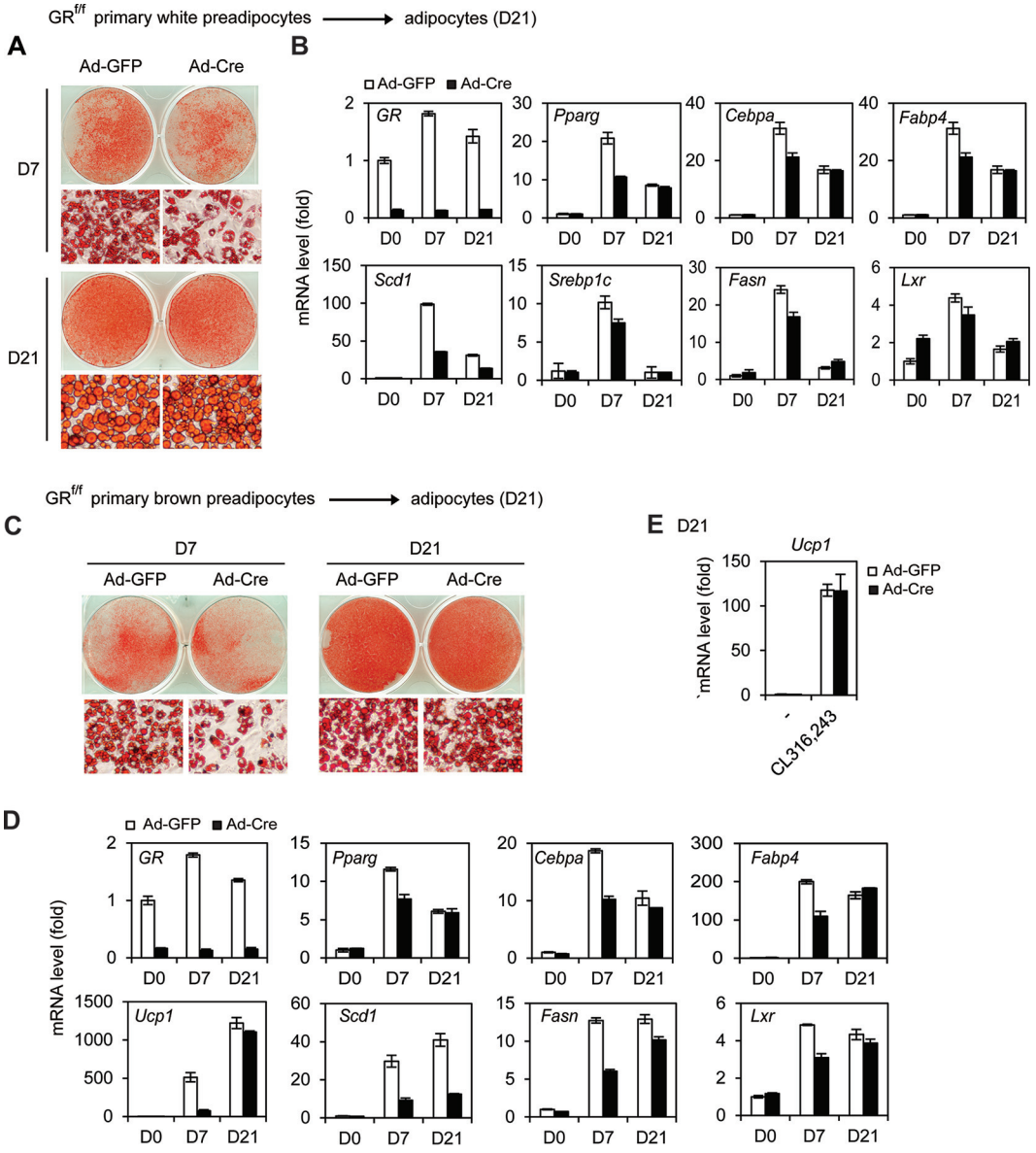

FIG 6 GR accelerates, but is dispensable for, adipogenesis in primary preadipocytes. (A, B) $GR^{f/f}$ primary white preadipocytes were infected with Ad-GFP or Ad-Cre, followed by white adipogenesis assays until D7 or D21. (A) Oil Red O staining of differentiated cells. (B) qRT-PCR analysis of adipogenesis markers *Pparγ*, *Cebpα*, and *Fabp4* as well as lipogenic genes *Scd1*, *Srebp1c*, *Fasn*, and *Lxr*. (C to E) $GR^{f/f}$ primary brown preadipocytes were infected with Ad-GFP or Ad-Cre, followed by adipogenesis until D7 or D21. (C) Oil Red O staining of differentiated cells. (D) qRT-PCR analysis of *GR*, adipogenesis markers, BAT markers, and lipogenic genes. (E) D21 mature brown adipocytes were treated with 100 nM CL-316,243 for 4 h. The induction of *Ucp1* expression was analyzed by qRT-PCR.

GR promotes adipogenesis in culture is by directly activating the expression of multiple adipogenic TFs.

GR recruits H3K27 acetyltransferase CBP to promote activation of C/EBPβ-primed enhancers. To understand how GR activates adipogenic gene expression in the early phase of adipogenesis, we performed ChIP-seq of GR, enhancer mark H3K4me1, and active enhancer mark H3K27ac at 4 h. We obtained 2,231 high-confidence GR binding regions (peaks) that were shared by two biological replicates. Among the 2,231 high-confidence GR binding regions, 1,995 (89.4%) were located on active enhancers while only 76 (3.4%) and 84 (3.7%) were located on promoters and primed enhancers, respectively (Fig. 9A). Motif analysis of GR binding regions at 4 h identified not only the motif of GR but also the motifs for C/EBPβ and CREB, among

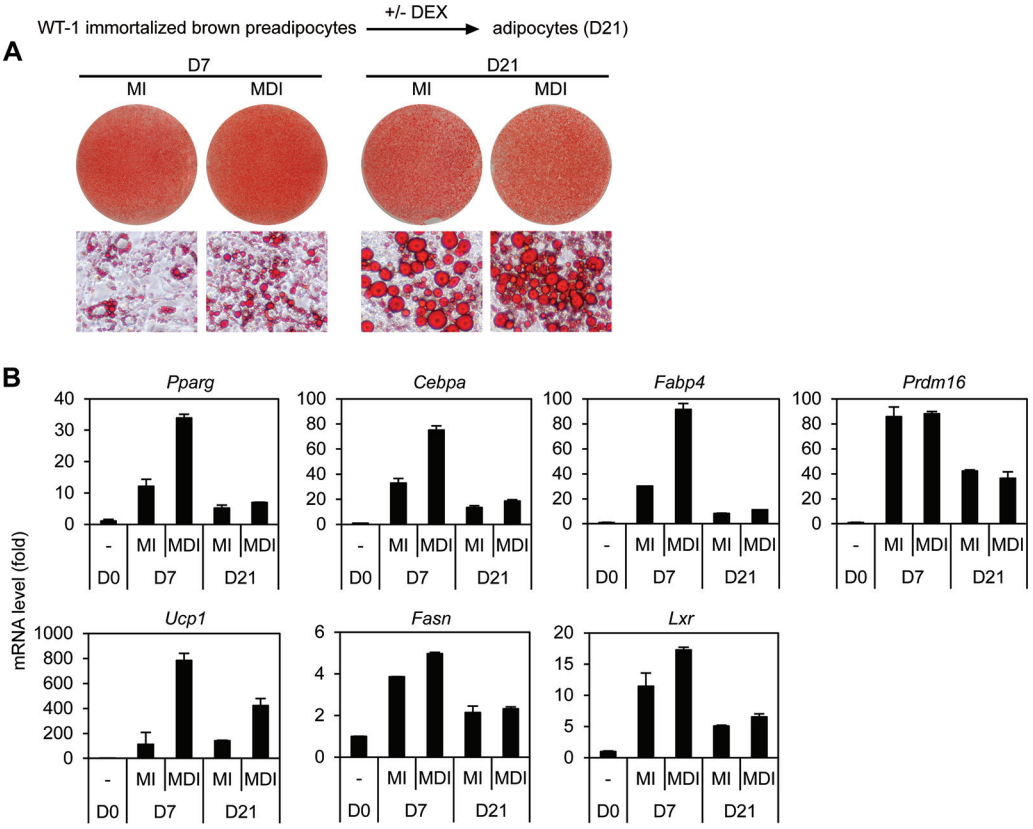

FIG 7 DEX accelerates, but is dispensable for, adipogenesis in culture. Adipogenesis was induced by treating the immortalized wild-type brown preadipocyte cell line WT-1 with the adipogenic cocktail with DEX (MDI) or without DEX (MI). (A) Oil Red O staining of differentiated adipocytes at D21. (B) qRT-PCR analysis of adipogenesis markers as well as lipogenic genes.

others (Fig. 9B). To experimentally validate the predicted motifs, we performed ChIP-seq of C/EBPβ and p-CREB at 4 h of adipogenesis. Consistent with the motif analysis and previous reports (7, 8), 2,078 (93.1%) and 951 (42.6%) of GR binding regions overlapped those of C/EBPβ and p-CREB at 4 h, respectively (Fig. 9C). Heat maps confirmed the colocalization of GR with C/EBPβ, p-CREB, H3K4me1, and H3K27ac on the 1,995 GR$^+$ active enhancers (Fig. 9D). Deletion of *GR* slightly decreased the binding of C/EBPβ but not p-CREB at GR$^+$ active enhancers (Fig. 9E).

Further ChIP-seq analysis of H3K27ac in *GR* KO and control cells revealed marked GR-dependent increases of H3K27ac on GR$^+$ active enhancers from 0 h to 4 h (Fig. 9F), indicating GR-dependent enhancer activation in the early phase of adipogenesis. Consistently, ChIP-seq revealed GR-dependent recruitment of the H3K27 acetyltransferase and transcription coactivator CBP on GR$^+$ active enhancers from 0 h to 4 h (Fig. 9G). On the *Cebp*δ locus, deletion of *GR* led to marked decreases of CBP and H3K27ac signals at distal downstream enhancer regions where GR colocalized with C/EBPβ and p-CREB (Fig. 9H). Together, these results indicate that GR activates expression of early adipogenic genes by recruiting H3K27 acetyltransferase CBP to promote activation of C/EBPβ-primed enhancers.

DISCUSSION

In this paper, we report that (i) GR is largely dispensable for BAT development and function in mice, (ii) DEX-mediated activation of GR accelerates, but is dispensable for, adipogenesis and induction of master adipogenic TFs in culture, (iii) the GR ligand DEX accelerates, but is dispensable for, adipogenesis in culture, (iv) DEX-bound GR directly promotes the expression of adipogenic TFs, including C/EBPβ, C/EBPδ, Klf5, Klf9, C/EBPα, and PPARγ in the early phase of differentiation, and (v) GR recruits H3K27

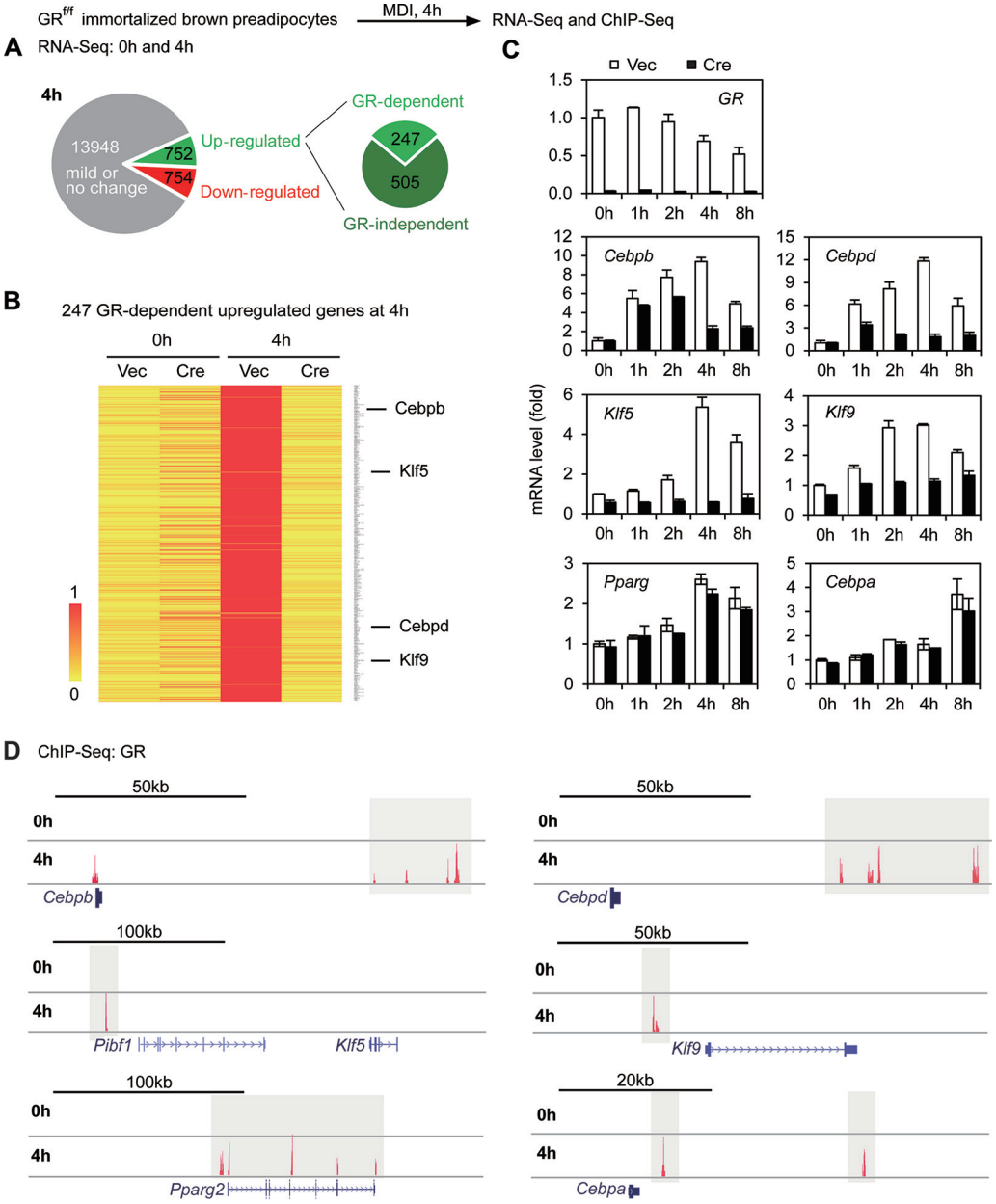

FIG 8 GR directly activates expression of multiple adipogenic TFs. *GR*$^{f/f}$ immortalized brown preadipocytes were infected with MSCVpuro expressing Cre. Cells were collected at 0 h and 4 h after induction of adipogenesis for RNA-Seq. (A) Schematic of identification of GR-dependent and -independent upregulated genes at 4 h. The threshold for up- or downregulation is 2.5-fold. (B) Heat map showing expression changes of the 247 GR-dependent upregulated genes from 0 h to 4 h. (C) qRT-PCR confirmation of GR-dependent upregulation of *C/EBPβ*, *C/EBPδ*, *Klf5*, *Klf9*, *Cebpα*, and *Pparγ* genes in the early phase of adipogenesis. (D) ChIP-Seq profiles of GR binding on gene loci encoding adipogenic TFs at 4 h.

acetyltransferase CBP to promote activation of C/EBPβ-primed enhancers of adipogenic genes. Consistent with our observations from adipogenesis of mouse preadipocytes, it has been shown that extensive adipogenesis of rat preadipocytes does not require the addition of DEX or other glucocorticoids (13, 14). It is also worth noting that our finding that GR is dispensable for adipogenesis is not at odds with the known role of GR in regulating lipogenesis in mature adipocytes (15).

We confirmed the previous report that knockdown of *GR* in 3T3-L1 cells impairs adipogenesis at day 8 (7). However, when we extended 3T3-L1 differentiation to 21 days, we found that DEX-bound GR accelerates, but is largely dispensable for, adipogenesis. We observed reduced lipid accumulation in brown and white adipocytes

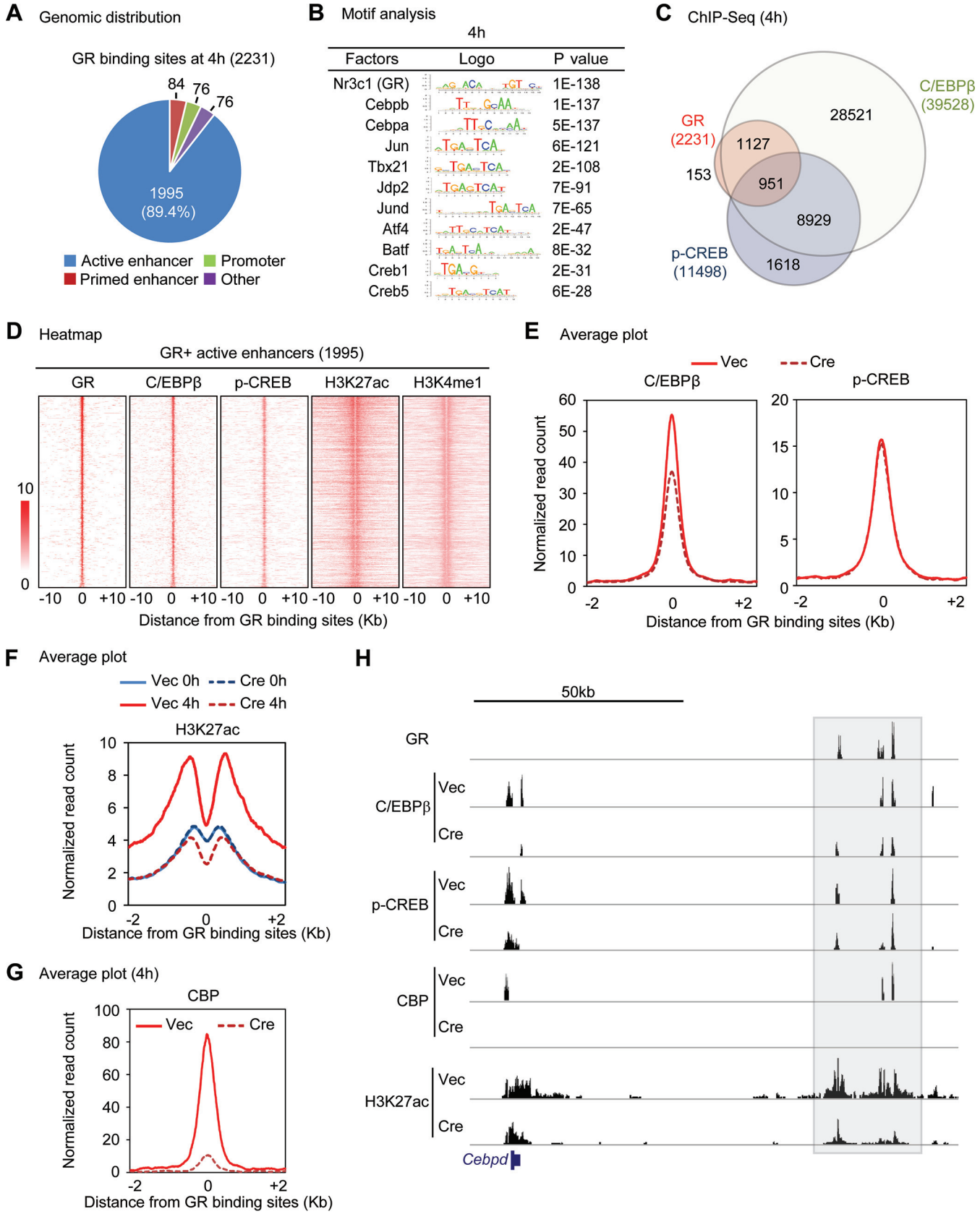

FIG 9 GR recruits H3K27 acetyltransferase CBP to promote activation of C/EBPβ-primed enhancers. (A to E) ChIP-seq analysis of GR, C/EBPβ, phospho-CREB (p-CREB), H3K4me1, and H3K27ac at 4 h after induction of adipogenesis in $GR^{f/f}$ immortalized brown preadipocytes. (A) Pie chart depicting the genomic distribution of GR binding regions. Of 2,231 GR biding regions, 1,995 (89.4%) are located on active enhancers. (B) Motif analysis of GR binding regions. (C) Venn

(Continued on next page)

derived from immortalized cells even after 21 days of differentiation, which is likely due to the reduced expression of lipogenic genes such as *Scd1*, *Fasn*, and *Lxr* in GR-depleted cells. However, when we induced adipogenesis in primary preadipocytes for 21 days, we observed levels of *Fasn* and *Lxr* expression and lipid accumulation that were similar to those in *GR* KO and wild-type cells. These results suggest that primary cells may better represent physiological adipogenesis.

The cellular functions of glucocorticoids are mediated by two nuclear receptors, GR and mineralocorticoid receptor (MR, also known as Nr3c2). An earlier study showed reduced differentiation potential of *MR* KO primary brown preadipocytes compared to the wild-type cells, although it was unclear whether the differentiation defect was due directly to the loss of *MR* or was secondary to the developmental defect of *MR* KO embryos (9). Our RNA-Seq data showed that unlike the substantial *GR* mRNA levels (RPKM $>$ 20), *MR* levels were extremely low (RPKM $<$ 0.2) throughout adipogenesis and were not affected by *GR* KO (Fig. 4D and E). These data suggest that GR plays a dominant role in mediating the adipogenic effects of glucocorticoids during adipogenesis and that MR is unlikely to compensate for the loss of GR.

Our observation that GR is dispensable for BAT development *in vivo* is consistent with our cell culture data. While GR is dispensable for BAT development, the $>$2-fold-decreased expression of a small number of genes in *GR* KO E18.5 BATs suggests that GR could be involved in regulating a subset of functions in BAT. For example, the expression levels of cold-induced genes *Dio2* and *Elovl3* but not *Ucp1* were moderately reduced by *GR* deletion in adult mice and embryos (Fig. 1L and 2B). However, *Ucp1* is critical for maintaining body temperature while deletion of *Dio2* or *Elovl3* does not significantly affect the body temperature in mice upon acute cold exposure (16–18). Consistently, *GR* cKO mice maintain normal body temperatures and display a behavior similar to that of control mice in the cold tolerance test. Together, our results suggest that GR is largely dispensable for BAT function in mice.

It was shown before that DEX-bound GR directly binds and activates the expression of *Cebp*δ and *Ppar*γ in the early phase of adipogenesis (7, 19, 20). We show that in addition, DEX-bound GR directly promotes the expression of adipogenic TFs, including C/EBPβ, Klf5, Klf9, and C/EBPα, in the early phase of adipogenesis. Consistent with previous reports for 3T3-L1 cells (7, 8), we found that the C/EBP binding motif is highly enriched at high-confidence GR binding sites in brown preadipocytes treated with DEX. The motif of activator protein 1 (AP1) is also highly enriched in GR binding regions in DEX-treated brown preadipocytes. AP1 is critical for GR-regulated transcription and GR recruitment to regulatory elements (1). While C/EBPβ is known to be important for GR target gene expression in the early phase of adipogenesis, future work is needed to find out the role of AP1 in regulating GR binding to and activation of adipogenic TF genes during adipogenesis.

MATERIALS AND METHODS

Plasmids and antibodies. Retroviral plasmids MSCVhygro-Cre, MSCVpuro-Cre, MSCVpuro-PPARγ, and pWZLhygro-C/EBPβ have been described previously (21–23). The lentiviral shRNA plasmid pLKO.1 targeting mouse *GR* (clone ID TRCN0000238463) and shRNA control plasmid were from Sigma. Anti-GR (sc-1004), anti-C/EBPβ (sc-150X), and anti-PPARγ (sc-7196X) antibodies were from Santa Cruz. Anti-RbBP5 antibody (A300-109A) was from Bethyl Laboratories. Anti-H3K27ac (ab4729) and anti-H3K4me1 (ab8895) antibodies were from Abcam. Anti-p-CREB antibody (catalog number CS204400) was from Millipore. Anti-CBP antibody (catalog number 7389) was from Cell Signaling.

Mouse experiments. $GR^{f/f}$ mice (24) (Jackson no. 021021) were crossed with *Myf5-Cre* mice (Jackson no. 007893). Histology and immunohistochemistry analyses of E18.5 embryos were done as described previously (22). For the cold tolerance test, individual mice were housed at 4°C as described previously (21). Body temperature was measured every hour for 5 h using a mouse rectal probe (Thermalert TH-5).

FIG 9 Legend (Continued)
diagram showing genomic colocalization of GR with C/EBPβ and p-CREB. (D) Heat maps showing genomic colocalization of C/EBPβ, p-CREB, H3K4me1, and H3K27ac with GR on 1,995 GR^+ active enhancers as defined for panel A. (E) Average profiles of C/EBPβ and p-CREB binding around the center of GR binding active enhancers at 4 h. (F and G) ChIP-seq analyses of H3K27ac and CBP at 4 h after induction of adipogenesis in $GR^{f/f}$ preadipocytes infected with retroviral Vec or Cre. Average binding profiles of H3K27ac (F) and CBP (G) around the center of GR binding active enhancers are shown. (H) Genome browser view of GR, C/EBPβ, p-CREB, and CBP binding as well as H3K27ac on *Cebp*δ locus in Vec and Cre cells.

At the end of the experiments, mice were euthanized and BATs were collected. Data were presented as means ± standard errors of the means (SEM). Differences were analyzed with Student's *t* test. All mouse work was approved by the Animal Care and Use Committee of NIDDK, NIH.

Isolation of primary preadipocytes, immortalization, virus infection, and adipogenesis assay. Primary brown preadipocytes were isolated from interscapular BAT of newborn $GR^{f/f}$ pups. Primary white adipocytes were from inguinal WAT of $GR^{f/f}$ adult mice. Immortalization of primary brown preadipocytes by retroviral vectors expressing SV40T was done as described previously (25, 26). SV40T inhibits adipogenesis of white but not brown preadipocytes (27). Cells were routinely cultured in Dulbecco's modified Eagle medium (DMEM) plus 10% fetal bovine serum (FBS). Retrovirus and adenovirus infections of preadipocytes were done as described previously (21).

Adipogenesis of immortalized white preadipocyte cell line 3T3-L1 was carried out as described previously (23). Briefly, confluent cells were exposed to the adipogenic cocktail containing 0.5 mM IBMX, 1 μM DEX, and 5 μg/ml insulin. After 2 days, cells were maintained in culture medium containing 5 μg/ml insulin until RNA collection or Oil Red O staining at day 7 (D7), D14, and D21. For adipogenesis of primary white preadipocytes, the same protocol was used, except that 1 μM rosiglitazone was included throughout the differentiation.

For brown adipogenesis assays, preadipocytes were plated at a density of 1×10^5 in each well of 6-well plates in growth medium (DMEM plus 10% FBS) 4 days before induction of adipogenesis. At day 0, cells were fully confluent and were treated with differentiation medium (DMEM plus 10% FBS, 0.1 μM insulin, and 1 nM T3) supplemented with 0.5 mM IBMX, 1 μM DEX, and 0.125 mM indomethacin. Two days later, cells were changed to the differentiation medium. The medium was replenished at 2-day intervals. Fully differentiated cells were either stained with Oil Red O or subjected to gene expression analysis by qRT-PCR.

qRT-PCR. Total RNA was extracted using TRIzol (Life Technologies) and reverse transcribed using ProtoScript II first-strand cDNA synthesis kit (New England BioLabs), following the manufacturers' instructions. qRT-PCR was done using the following SYBR green primers: *GR*, forward, 5′-CGTGTGGAAG CTGTAAAGTCTTCTT-3′, and reverse, 5′-CTTCGAATTTTATCAATGATGCAATC-3′; *Scd1*, forward, 5′-TTCTTG CGATACACTCTGGTGC-3′, and reverse, 5′-CGGGATTGAATGTTCTTGTCGT-3′; *Srebp1c*, forward, 5′-GGCAC TAAGTGCCCTCAACCT-3′, and reverse, 5′-GCCACATAGATCTCTGCCAGTGT-3′; *Fasn*, forward, 5′-TGTGGAC ATGGTCACAGATG-3′, and reverse, 5′-CGTCGAACTTGGAGAGATCC-3′; *Lxr*, forward, 5′-CTCAATGCCTGAT GTTTCTCCT-3′, and reverse, 5′-TCCAACCCTATCCCTAAAGCAA-3′. SYBR green primers for other genes were described previously (28).

RNA-Seq. RNA-Seq was done using immortalized $GR^{f/f}$ preadipocytes according to the protocol described previously (22). We collected reads (single end, 50 bp) that aligned with sequences annotated in the Build 37 assembly of the NCBI mouse genome data (NCBI37/mm9), and then each gene expression level was calculated in units of reads per kilobase per million (RPKM). We compared the mRNA levels in Cre- and in Vec-infected $GR^{f/f}$ cells and set the fold change cutoff to 2.5 to identify upregulated and downregulated genes. We defined GR-dependent genes as those with over a 2.5-fold downregulation in GR-deficient cells (Cre) compared to control cells (Vec). The gene ontology (GO) study was carried out using DAVID (29) with the whole genome as the background.

ChIP and ChIP-seq. ChIP and ChIP-seq were done as described previously (22). For each ChIP, 4 to 10 μg of antibodies was used. The final libraries were sequenced on Illumina HiSeq 2500. GR, C/EBPβ, p-CREB, and H3K27ac ChIP-Seq assays were performed in duplicates. Identification of ChIP-enriched regions was performed using the island approach "SICER" (30). Read numbers for the resulting peaks were quantified and normalized to total mapped reads. For GR, C/EBPβ, and p-CREB ChIP-seq data sets, the window size was chosen to be 50 bp and the false-discovery rate (FDR) threshold was set to be 10^{-10}. We took only common regions that were shared between the two biological replicates into consideration when selecting high-confidence binding regions. We obtained a total of 2,231 high-confidence GR peaks, 39,528 high-confidence C/EBPβ peaks, and 11,498 high-confidence p-CREB peaks. For the ChIP-seq data sets of histone modifications (H3K4me1 and H3K27ac), the window size was chosen to be 200 bp and the FDR threshold was chosen to be 10^{-3}. A motif search around the GR binding regions was conducted using SeqPos (31). Sequencing results were visualized in UCSC Genome Browser.

To identify the genomic distribution of GR binding regions, we performed H3K4me1 and H3K27ac ChIP-seq and classified them into one of the four types of gene-regulatory elements using 2,231 high-confidence GR binding regions. We first determined whether they were promoters ($H3K4me1^-$), enhancers ($H3K4me1^+$), or others and then further narrowed them down to either active ($H3K4me1^+$ $H3K27ac^+$) or primed ($H3K4me1^+$ $H3K27ac^-$) enhancers. Regions within ±1 kb of the transcription start site (TSS) were treated as promoters in this study. Average profiles were plotted using the number of ChIP-seq reads (normalized to the size of each library) in 5-bp bins from the center of the GR binding active enhancer regions within 2 kb on both sides. The heat maps were generated with 50-bp resolution and ranked according to the colocalization of C/EBPβ and p-CREB binding sites.

Statistical analyses. To compare between two groups, the statistical significance was calculated using the two-tailed unpaired *t* test on two experimental conditions. A *P* value of less than 0.05 was considered statistically significant.

Accession number. All data sets described in this paper, including 8 RNA-Seq samples, 20 ChIP-seq samples, and 4 ChIP-seq inputs, have been deposited in NCBI Gene Expression Omnibus under accession number GSE76619.

ACKNOWLEDGMENT

We thank Jonathan Ashwell for the $GR^{f/f}$ mice, Philippe Soriano for the *Myf5-Cre* mice, Yu-Hua Tseng for the wild-type brown preadipocyte cell line, and NIDDK Genomics Core for sequencing.

This work was supported by the Intramural Research Program of NIDDK, NIH, to K.G.

REFERENCES

1. Biddie SC, John S, Sabo PJ, Thurman RE, Johnson TA, Schiltz RL, Miranda TB, Sung M-H, Trump S, Lightman SL, Vinson C, Stamatoyannopoulos JA, Hager GL. 2011. Transcription factor AP1 potentiates chromatin accessibility and glucocorticoid receptor binding. Mol Cell 43:145–155. https://doi.org/10.1016/j.molcel.2011.06.016.
2. Gregoire FM, Smas CM, Sul HS. 1998. Understanding adipocyte differentiation. Physiol Rev 78:783–809.
3. Rubin CS, Hirsch A, Fung C, Rosen OM. 1978. Development of hormone receptors and hormonal responsiveness in vitro. Insulin receptors and insulin sensitivity in the preadipocyte and adipocyte forms of 3T3-L1 cells. J Biol Chem 253:7570–7578.
4. Student AK, Hsu RY, Lane MD. 1980. Induction of fatty acid synthetase synthesis in differentiating 3T3-L1 preadipocytes. J Biol Chem 255:4745–4750.
5. Farmer SR. 2006. Transcriptional control of adipocyte formation. Cell Metab 4:263–273. https://doi.org/10.1016/j.cmet.2006.07.001.
6. Yeh WC, Cao Z, Classon M, McKnight SL. 1995. Cascade regulation of terminal adipocyte differentiation by three members of the C/EBP family of leucine zipper proteins. Genes Dev 9:168–181. https://doi.org/10.1101/gad.9.2.168.
7. Steger DJ, Grant GR, Schupp M, Tomaru T, Lefterova MI, Schug J, Manduchi E, Stoeckert CJ, Lazar MA. 2010. Propagation of adipogenic signals through an epigenomic transition state. Genes Dev 24:1035–1044. https://doi.org/10.1101/gad.1907110.
8. Siersbaek R, Nielsen R, John S, Sung MH, Baek S, Loft A, Hager GL, Mandrup S. 2011. Extensive chromatin remodelling and establishment of transcription factor 'hotspots' during early adipogenesis. EMBO J 30:1459–1472. https://doi.org/10.1038/emboj.2011.65.
9. Hoppmann J, Perwitz N, Meier B, Fasshauer M, Hadaschik D, Lehnert H, Klein J. 2010. The balance between gluco- and mineralo-corticoid action critically determines inflammatory adipocyte responses. J Endocrinol 204:153–164. https://doi.org/10.1677/JOE-09-0292.
10. Cristancho AG, Lazar MA. 2011. Forming functional fat: a growing understanding of adipocyte differentiation. Nat Rev Mol Cell Biol 12:722–734. https://doi.org/10.1038/nrm3198.
11. Seale P, Bjork B, Yang W, Kajimura S, Chin S, Kuang S, Scime A, Devarakonda S, Conroe HM, Erdjument-Bromage H, Tempst P, Rudnicki MA, Beier DR, Spiegelman BM. 2008. PRDM16 controls a brown fat/skeletal muscle switch. Nature 454:961–967. https://doi.org/10.1038/nature07182.
12. Lee JE, Ge K. 2014. Transcriptional and epigenetic regulation of PPARgamma expression during adipogenesis. Cell Biosci 4:29. https://doi.org/10.1186/2045-3701-4-29.
13. Deslex S, Negrel R, Ailhaud G. 1987. Development of a chemically defined serum-free medium for differentiation of rat adipose precursor cells. Exp Cell Res 168:15–30. https://doi.org/10.1016/0014-4827(87)90412-5.
14. Gregoire F, Todoroff G, Hauser N, Remacle C. 1990. The stroma-vascular fraction of rat inguinal and epididymal adipose tissue and the adipoconversion of fat cell precursors in primary culture. Biol Cell 69:215–222. https://doi.org/10.1016/0248-4900(90)90348-7.
15. Wang JC, Gray NE, Kuo T, Harris CA. 2012. Regulation of triglyceride metabolism by glucocorticoid receptor. Cell Biosci 2:19. https://doi.org/10.1186/2045-3701-2-19.
16. Christoffolete MA, Linardi CC, de Jesus L, Ebina KN, Carvalho SD, Ribeiro MO, Rabelo R, Curcio C, Martins L, Kimura ET, Bianco AC. 2004. Mice with targeted disruption of the Dio2 gene have cold-induced overexpression of the uncoupling protein 1 gene but fail to increase brown adipose tissue lipogenesis and adaptive thermogenesis. Diabetes 53:577–584. https://doi.org/10.2337/diabetes.53.3.577.
17. Westerberg R, Mansson JE, Golozoubova V, Shabalina IG, Backlund EC, Tvrdik P, Retterstol K, Capecchi MR, Jacobsson A. 2006. ELOVL3 is an important component for early onset of lipid recruitment in brown adipose tissue. J Biol Chem 281:4958–4968. https://doi.org/10.1074/jbc.M511588200.
18. Enerback S, Jacobsson A, Simpson EM, Guerra C, Yamashita H, Harper ME, Kozak LP. 1997. Mice lacking mitochondrial uncoupling protein are cold-sensitive but not obese. Nature 387:90–94. https://doi.org/10.1038/387090a0.
19. MacDougald OA, Cornelius P, Lin FT, Chen SS, Lane MD. 1994. Glucocorticoids reciprocally regulate expression of the CCAAT/enhancer-binding protein alpha and delta genes in 3T3-L1 adipocytes and white adipose tissue. J Biol Chem 269:19041–19047.
20. Siersbaek R, Baek S, Rabiee A, Nielsen R, Traynor S, Clark N, Sandelin A, Jensen ON, Sung MH, Hager GL, Mandrup S. 2014. Molecular architecture of transcription factor hotspots in early adipogenesis. Cell Rep 7:1434–1442. https://doi.org/10.1016/j.celrep.2014.04.043.
21. Cho YW, Hong S, Jin Q, Wang L, Lee JE, Gavrilova O, Ge K. 2009. Histone methylation regulator PTIP is required for PPARgamma and C/EBPalpha expression and adipogenesis. Cell Metab 10:27–39. https://doi.org/10.1016/j.cmet.2009.05.010.
22. Lee JE, Wang C, Xu S, Cho YW, Wang L, Feng X, Baldridge A, Sartorelli V, Zhuang L, Peng W, Ge K. 2013. H3K4 mono- and di-methyltransferase MLL4 is required for enhancer activation during cell differentiation. Elife 2:e01503. https://doi.org/10.7554/eLife.01503.
23. Wang L, Xu S, Lee J-E, Baldridge A, Grullon S, Peng W, Ge K. 2013. Histone H3K9 methyltransferase G9a represses PPAR[gamma] expression and adipogenesis. EMBO J 32:45–59. https://doi.org/10.1038/emboj.2012.306.
24. Mittelstadt PR, Monteiro JP, Ashwell JD. 2012. Thymocyte responsiveness to endogenous glucocorticoids is required for immunological fitness. J Clin Invest 122:2384–2394. https://doi.org/10.1172/JCI63067.
25. Klein J, Fasshauer M, Ito M, Lowell BB, Benito M, Kahn CR. 1999. beta 3-Adrenergic stimulation differentially inhibits insulin signaling and decreases insulin-induced glucose uptake in brown adipocytes. J Biol Chem 274:34795–34802. https://doi.org/10.1074/jbc.274.49.34795.
26. Wang L, Jin Q, Lee JE, Su IH, Ge K. 2010. Histone H3K27 methyltransferase Ezh2 represses Wnt genes to facilitate adipogenesis. Proc Natl Acad Sci U S A 107:7317–7322. https://doi.org/10.1073/pnas.1000031107.
27. Hansen JB, Jørgensen C, Petersen RK, Hallenborg P, De Matteis R, Bøye HA, Petrovic N, Enerbäck S, Nedergaard J, Cinti S, Riele Ht, Kristiansen K. 2004. Retinoblastoma protein functions as a molecular switch determining white versus brown adipocyte differentiation. Proc Natl Acad Sci U S A 101:4112–4117. https://doi.org/10.1073/pnas.0301964101.
28. Jin Q, Wang C, Kuang X, Feng X, Sartorelli V, Ying H, Ge K, Dent SY. 2014. Gcn5 and PCAF regulate PPARgamma and Prdm16 expression to facilitate brown adipogenesis. Mol Cell Biol 34:3746–3753. https://doi.org/10.1128/MCB.00622-14.
29. Huang DW, Sherman BT, Lempicki RA. 2009. Systematic and integrative analysis of large gene lists using DAVID bioinformatics resources. Nat Protoc 4:44–57. https://doi.org/10.1038/nprot.2008.211.
30. Zang C, Schones DE, Zeng C, Cui K, Zhao K, Peng W. 2009. A clustering approach for identification of enriched domains from histone modification ChIP-Seq data. Bioinformatics 25:1952–1958. https://doi.org/10.1093/bioinformatics/btp340.
31. He HH, Meyer CA, Shin H, Bailey ST, Wei G, Wang Q, Zhang Y, Xu K, Ni M, Lupien M, Mieczkowski P, Lieb JD, Zhao K, Brown M, Liu XS. 2010. Nucleosome dynamics define transcriptional enhancers. Nat Genet 42:343–347. https://doi.org/10.1038/ng.545.